MATHEMATICAL MODELING OF COLD CAP: EFFECT OF BUBBLING ON MELTING RATE

#RICHARD POKORNY*, ALBERT A. KRUGER**, PAVEL HRMA***

**Department of Chemical Engineering, Institute of Chemical Technology in Prague, Technicka 5, 166 28 Prague 6, Czech Republic*
***U.S. Department of Energy, Office of River Protection, 2440 Stevens Dr., Richland, WA 99352, USA*
****Pacific Northwest National Laboratory, P.O. Box 999, Richland ,WA 99352, USA*

#E-mail: Richard.Pokorny@vscht.cz

Submitted October 26, 2014; accepted December 22, 2014

Keywords: Glass melting, Glass foaming, Waste vitrification, Cold cap, Bubbling

The rate of melting is a primary concern in the vitrification of radioactive wastes because it directly influences the life cycle of nuclear waste cleanup efforts. To increase glass melting performance, experimental and industrial all-electric waste glass melters employ various melt-rate enhancement techniques, the most prominent being the application of bubblers submerged into molten glass. This study investigates various ways in which bubbling affects melting rate in a waste glass melter. Using the recently developed cold cap model, we suggest that forced convection of molten glass, which increases the cold cap bottom temperature, is the main factor. Other effects, such as stirring the feed into molten glass or reducing the insulating effect of foaming, also play a role.

INTRODUCTION

More than 200,000 m^3 of nuclear waste glass will be vitrified over the next decades at the U.S. Department of Energy's (DOE) Hanford Site in southeastern Washington State, USA [1]. The vitrification will be performed in an all-electric (Joule-heated) waste glass melter, which is shown schematically in Figure 1. The feed slurry (the term "melter feed" is used for what commercial glass makers call "glass batch") is charged to the melter from above, forming a reacting layer on the pool of molten glass. In this layer, called a "cold cap", most of the feed-to-glass conversion occurs. The electrical current from the electrodes delivers the heat for melting, while bubbling increases heat transfer to the cold cap via forced convection within the melt.

As discussed in Pokorny and Hrma [2], a foam layer separates the main reaction layer in the cold cap from the molten glass. This foam layer, shown in Figure 2, consists of three sublayers: primary foam, gas cavities, and secondary foam. Primary foam is generated at temperature, T_P, at which the glass forming melt

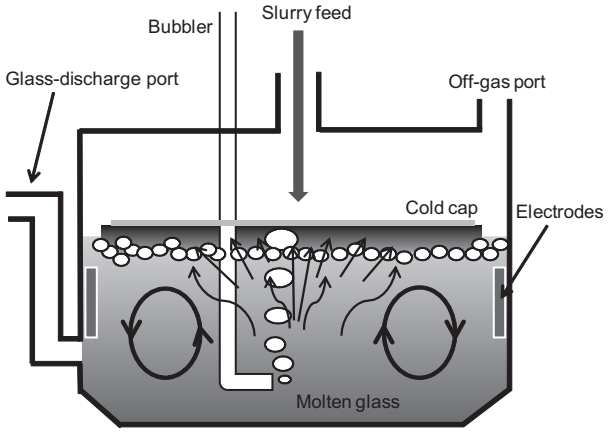

Figure 1. Schematic illustration of a Joule-heated waste glass melter.

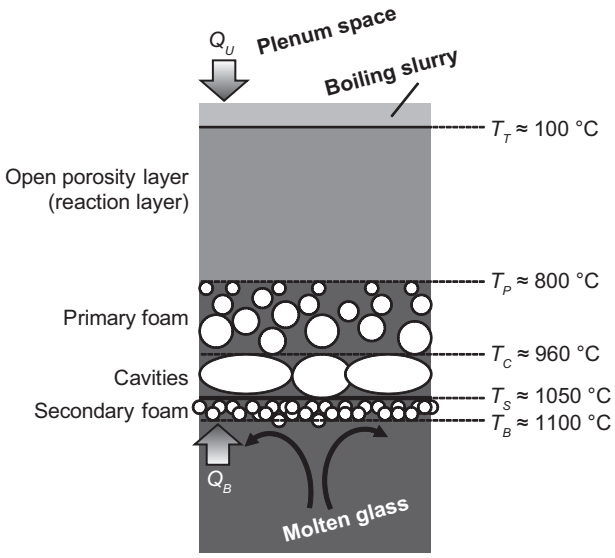

Figure 2. Schematic of the cold cap illustrating individual cold cap layers, boundary temperatures, and heat fluxes from the plenum space, Q_U, and from molten glass, Q_B.

connects and open porosity closes, trapping evolving gas in growing bubbles. Because of the high viscosity of the melt, the buoyant motion of the primary bubbles is slower than the downward motion of the melt. The primary bubbles thus descend until, at the cavity temperature, T_C, bubbles coalesce and merge with large cavities below. Cavities are sandwiched between primary and secondary foam produced by bubbles from the redox reactions in molten glass. Cavities releases gas into the plenum space on cold cap edges.

To enhance glass melting, bubblers have been used in the commercial glass-making industry for many decades [3]. In waste glass melters, bubblers located directly under the cold cap have a considerable boosting impact on the melting rate [4] as shown by data in Figure 3. These data were compiled from several melter runs with different feed compositions.

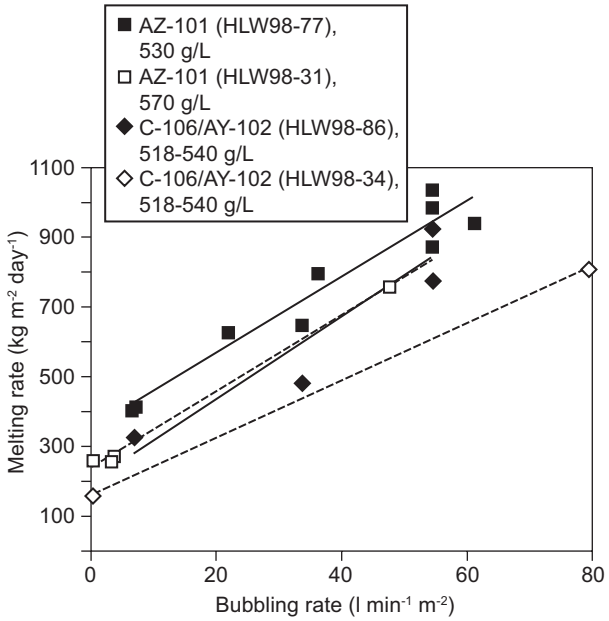

Figure 3. Melting rate versus bubbling rate for different feed compositions compiled from several reports issued by the Vitreous State Laboratory (VSL) for the DOE Office of River Protection [5]. The legend identifies the Hanford tank waste, the VSL glass designed for the waste, and the glass mass per slurry feed volume (Courtesy of Dong-Sang Kim).

According to a recent report [6], bubbling increased the melting rate to as high as 2200 kg m^{-2}·day^{-1}. This effect can be attributed to following factors:

1. Bubbling generates powerful forced convection in molten glass that greatly exceeds natural convection driven by buoyancy. As a result, velocity and temperature gradients below the cold cap become steeper. As the temperature at the cold cap bottom rises, more heat is delivered to the cold cap, thereby producing more glass per unit time and area.
2. Large bubbles from bubblers sweep secondary foam (see Figure 2) from beneath the cold cap, removing the insulating secondary foam layer from cold cap bottom, thus further increasing the transferred heat.
3. With strong bubbling, the cavity layer, into which the primary foam gas is released, can be displaced together with secondary foam (see Figure 2), exposing the primary foam to the upwelling hot glass. Primary foam then collapses faster, allowing more heat to be delivered to the cold cap.
4. Feed can be stirred into the melt at the edges of vent holes that open above the bubblers, exposing a fraction of the feed to high temperatures at which batch reactions are rapid and gases are quickly released if the viscosity is low enough.
5. Bubblers can increase the temperature above the cold cap by bringing hot gas to the plenum space and by exposing the plenum space to the hot melt in the vent holes. The augmented heat flux to the cold cap from the plenum space helps increase melting rate.

In the following section, we separately examine the melt-bubbling effects 1-3 and 5 using the cold cap model, which has been developed to simulate and optimize the performance of a Joule-heated melter for nuclear waste vitrification [2, 7]. This model solves simplified balances of mass and energy using the finite volume method. It estimates the melting rate of glass batches as a function of batch properties and melter operating conditions and incorporates the structure and dynamics of the insulating foam layer separating the cold cap and the molten glass. As to the fourth effect, Chapman [8] and Perez et al. [4] considered the stirring effect as the main melting-rate enhancing factor. However, as we show in the Result and Discussion section, recent data do not support this hypothesis.

RESULTS AND DICSUSSION

Effects of bubbling on melting rate

Forced convection

With enhanced convection induced by bubbling, velocity gradients under the cold cap become steeper, the thermal boundary layer is suppressed, and the temperature at the cold cap bottom, T_B, rises.
The melting rate, j_0, is proportional to the heat flux to the cold cap, Q, by the relationship [2]

$$j_0 = \frac{Q_U + Q_B}{H_{melt} + H_{slurry}} \tag{1}$$

where $H_{melt} = \int_{T_T}^{T_B} c_b^{Eff}\, dT$ is the heat necessary to raise dry feed temperature from the cold cap top temperature, T_T, to the cold cap bottom temperature, T_B; H_{slurry} is the heat to turn the slurry fed to the melter into dry feed at 100°C, Q_U is the heat flux from plenum space, and Q_B is

the heat flux from molten glass. According to the laws governing heat conduction and radiation, Q_B depends on the thickness and heat conductivity of each of the foam sublayers, and on the boundary temperatures, T_P, T_C, T_S, T_B, as indicated in Figure 2.

The cold cap bottom temperature, T_B, is a model parameter that can only be estimated using the model of the whole glass melter that is being developed at Idaho National Laboratory [9]. However, the primary foam temperature, T_P, and cavity temperature, T_C, can be obtained as minima and maxima on expansion curves, which relate the area or volume of dry feed pellets heated at a constant rate to temperature [2].

Figure 4 displays expansion curves for A0 feed formulated for a high-alumina waste glass [10]. This feed has been well characterized by experimental studies with respect to material properties at various stages of conversion [11, 12, 13] and conversion kinetics in response to various time-temperature histories [14, 15, 16]. The T_P, the temperature above which the open porosity closes, is identified as the deep minimum on the expansion curve. Above T_P, feed reaction gases are trapped in bubbles within the high-viscosity melt, creating primary foam. Primary foam collapses at T_C, a temperature identified as the first maximum on the expansion curve.

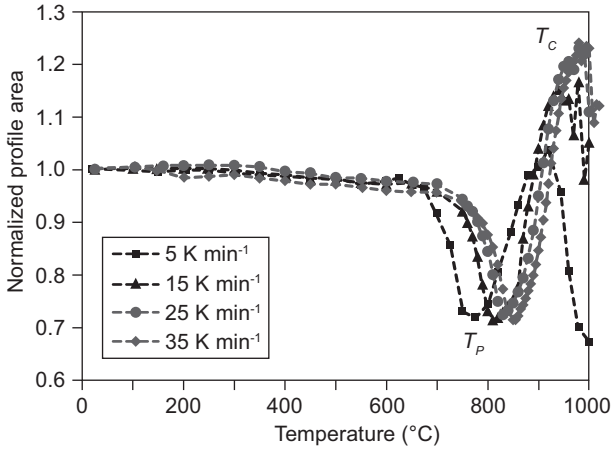

Figure 4. Normalized feed-pellet profile area versus temperature and heating rate (indicated in the legend).

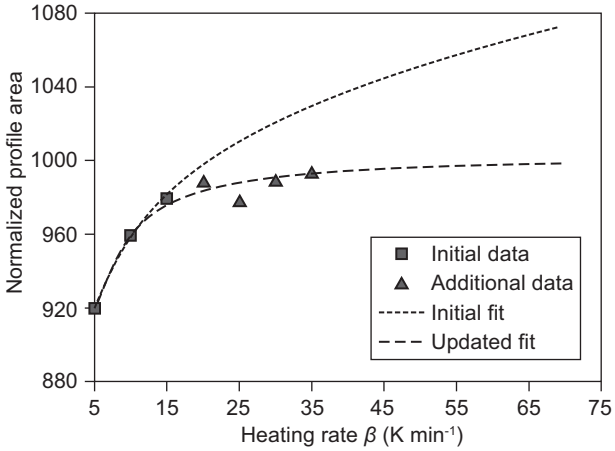

Figure 5. Primary foam collapsing temperature, T_C, versus heating rate.

Figure 5 displays two approximation functions for T_C versus heating rate, β, one fitted to initial data that were previously available only for $b \leq 15$ K·min^{-1} [2], and the other to an extended dataset obtained with an improved experimental setup that allowed measurements to be conducted at higher heating rates. The dotted line represents the initial function, $T_C = T_{C1}(\beta/\beta_1)^{\gamma}$, where b_1 is a reference heating rate, and T_{C1} and γ are constant coefficients. With $b_1 = 10$ K·min^{-1}, the coefficient values were $T_{C1} = 959$°C and $\gamma = 0.058$. The extended dataset was fitted by an updated function, $T_C = T_{C_2}[1 - (\beta/\beta_2)^{\lambda}]$, represented by the dashed line, with $b_2 = 0.467$ K min^{-1}, $T_{C_2} = 1019.9$°C, and $\lambda = -1.047$.

Because heating rates experienced by the feed within the cold cap can be as high as 70 K·min^{-1} [2], the $T_C(\beta)$ approximation functions were extrapolated beyond measured data. The initial approximation function (dotted line in Figure 5) showed dramatic increase of T_C at higher β values. However, such a strong increase is not expected, as heating rate has only little effect on melt viscosity, which determines when the foam becomes unstable. The extended dataset obtained at higher β is in agreement with this reasoning.

As Figure 6 shows, model calculations performed with the initial approximation function, which showed dramatic increase of T_C at higher β, led to a slow response of melting rate to increasing T_B. On the other hand, the milder increase of T_C with β values estimated with the updated function led to a stronger response of melting rate to increasing T_B (Figure 6), which agrees more closely with experimental observations. Clearly,

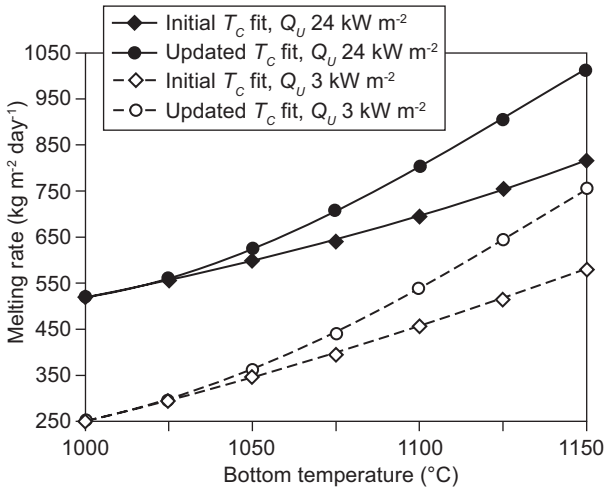

Figure 6. Response of melting rate to cold cap bottom temperature for two Q_U values (3 kW·m^{-2}, dashed lines, and 24 kW·m^{-2}, solid lines) calculated using the initial (diamonds) and updated (circles) $T_C(\beta)$ approximation functions.

when temperature T_C, at which primary foam collapses, increases mildly with heating rate, the higher difference between T_C and T_S allows the heat needed for faster melting to be transferred across the cavity layer.

As Figure 7 shows, the effect of the $T_C(\beta)$ approximation function on T_C is substantial. Figure 6 also shows that the heat supplied from the plenum space, Q_U, has a significant effect on melting rate. This will be discussed in section "Plenum space temperature and estimation of Q_U".

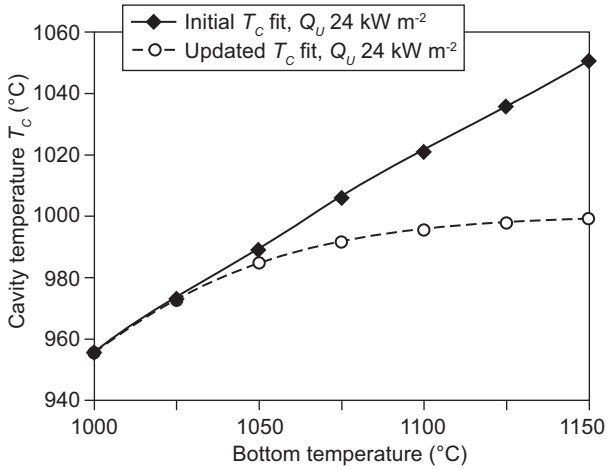

Figure 7. Primary foam collapsing temperature versus cold cap bottom temperature. Model-calculated result using initial (solid line) and updated (dashed line) $T_C(\beta)$ approximation function.

Regrettably, experimental observations of the exact cold cap bottom temperature are not practically feasible. Matlack et al. [17] report experimentally measured melt temperatures from the melter bottom in close proximity of the cold cap. With a melter operating temperature, T_M, of 1150°C, the thermocouple located below the cold cap measured temperatures that fluctuated around 900°C during the test without bubbling and ~ 1100°C during the test with bubbling. These data do not measure the actual T_B values but indicate that T_B values increase substantially and perhaps proportionally, in response to bubbling.

Secondary foam

Bubbles from redox reactions in molten glass accumulate under the cold cap and produce a secondary foam layer, the thickness of which can be expressed by the formula [18]

$$h_s = k\,\Phi\,j_M, \qquad (2)$$

where j_M is the melting rate and Φ is the foaminess, which is a coefficient that relates the extent of foaming to the superficial gas flow [19]. Typical values of Φ for glass are in the order of 10^2 s [18]. The coefficient k represents the amount of gas evolved per unit mass of molten glass [2].

Figure 8 and Figure 9 display the change of melting rate and secondary foam layer thickness with the cold cap bottom temperature for three values of Φ. The values Φ = 100 and Φ = 400 were chosen to cover the typical molten glass behavior, whereas a value of Φ = 1 was chosen for a limiting case of practically no secondary foaming. As expected, the melting rate decreases and the secondary foam thickness increases with increasing foaminess. This is a result of decreasing T_S with increasing Φ (Figure 10) and, thus, decreasing heat flux, Q_B, to the cold cap.

Secondary foam merges into cavities under the cold cap, which then opens into the plenum space on cold cap edges or in vent holes [2]. This finding is in agreement with the observation that only large bubbles periodically burst, but no fine bubbles of secondary foam emerge from beneath the cold cap even when bubblers are not used [5]. In a special case of extremely low foaminess, such as when Φ = 1, rising bubbles burst as soon as they reach melt surface, and the secondary foam thickness becomes negligible (Figure 9). This case

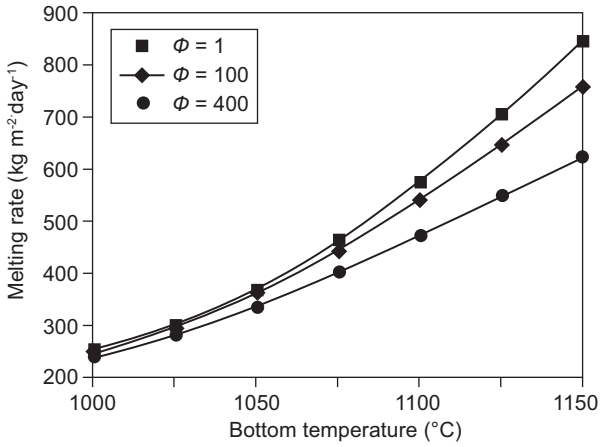

Figure 8. Melting rate versus cold cap bottom temperature for different values of foaminess (Φ, in s).

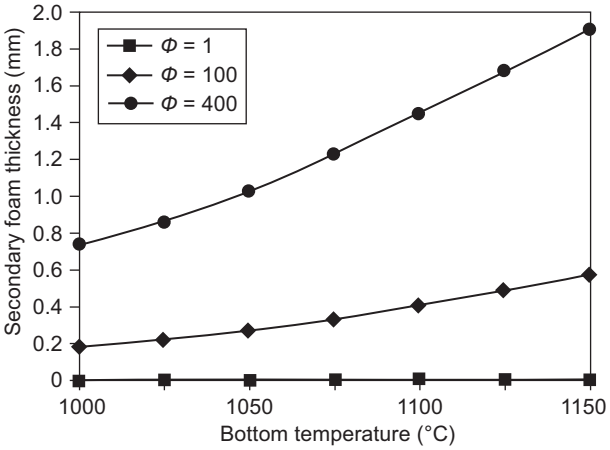

Figure 9. Secondary foam thickness versus cold cap bottom temperature for different values of foaminess (Φ, in s).

is equivalent to the situation in which small bubbles do not reach the surface because they are swept away with the current caused by bubbling. Then $T_S \approx T_B$ (Figure 10, $\Phi = 1$), so secondary foam presents little resistance to heat flow, and the melting rate increases (Figure 8). In reality, it is likely that the secondary foam is swept only partially. Thus, the actual dependence of melting rate on T_B for particular foaminess (for example $\Phi = 400$) will lie in the region bounded by lines $\Phi = 400$ (secondary foam not swept by bubbling) and $\Phi = 1$ (foam completely swept).

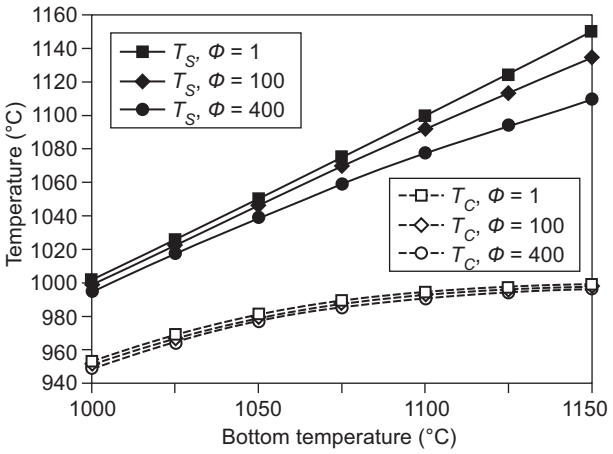

Figure 10. Cavity layer boundary temperatures T_C and T_S versus cold cap bottom temperature and foaminess (Φ, in s).

Direct contact of molten glass with primary foam

With vigorous bubbling, a situation may occur in which both secondary foam and cavities are displaced by bubbling and molten glass comes into direct contact with primary foam. Then $T_C = T_B$, and heat transfer from the molten glass to the unreacted feed in the cold cap intensifies. In this case, a modified model must be used to determine the melting rate.

Actually, earlier models of batch melting did not consider cavities and a secondary foam layer [20]. Instead, they assumed that melting rate is jointly controlled by the heat transfer to the cold cap and by the kinetics of the final stage of the feed-to-glass conversion process, or the "terminal batch-to-glass conversion rate," a term that is not well defined. We propose that the terminal conversion is identified as the expansion and collapse of primary foam [2, 21], starting when open pores close, progressing as the feed expands, and ending when bubbles collapse. At this point, the molten feed merges with the circulating glass melt below. Several models were developed in the past to model foam expansion and collapse [22, 23, 24]. A simple kinetic model, based on foam evolution curves shown in Figure 4, is currently being developed.

Mixing of the feed with the molten glass near vent holes

In their pioneering work, Chapman [8] and Perez et al. [4] claimed that large ascending bubbles effectively pump hot molten glass to the surface (Figure 11, right), stirring feed into molten glass in the so called "zones of influence" [8]. Using this assumption, they derived a linear relationship between the glass production rate and the melter bubbled area [4]

$$P_R = P_0 + C_1\, a_{bm} \tag{3}$$

where P_R is the production rate, P_0 is the production rate of unbubbled area, C is a coefficient, and a_{bm} is the fraction of melt surface area bubbled, which is defined as

$$a_{bm} = \frac{n_{noz}\, A_b\, F_{OL}}{A_m} \tag{4}$$

where n_{noz} is the number of nozzles in the melter; A_b is the bubbled area per nozzle, which is a function of bubbling rate; A_m is the melt surface area; and F_{OL} is the overlap factor ($F_{OL} \leq 1$). The F_{OL} term accounts for the overlap between the bubbled areas of two or more nozzles and with a refractory wall.

Though Equation 3 was successfully used for the optimization and design of bubbler configuration [4, 8], recent experiments do not confirm the mixing hypothesis. Additional bubbling outlets in a large-scale melter did not always result in the formations of openings in the cold cap above the added bubblers [25], while the melting rate still increased considerably. As Figure 11 illustrates, the gas bubbles from some bubblers may not possess sufficient buoyancy to burst through the cold cap. This suggests that the mixing of the molten glass with the feed around vent holes is not likely to be the dominant factor in the melting rate increase. Equation 3 rationalizes the linear trend seen in Figure 3 but does

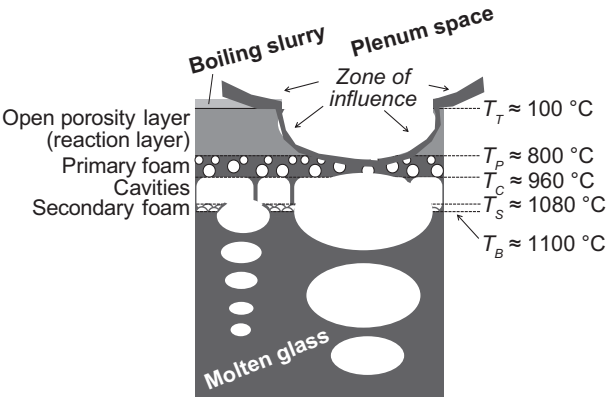

Figure 11. Schematic illustration of bubbles penetrating cold cap. On the right side, a large bubble from a bubbler possesses sufficient buoyancy to burst through the cold cap and create a vent hole. On the left side, a smaller bubble merges with gas cavities under the cold cap. In the "zone of influence" around the vent hole, hot molten glass is mixed with feed, thus speeding the conversion process.

not capture the complex mechanism of the bubbling effect. A mathematical model that is firmly based on physicochemical dynamics can account for multiple effects, provide better understanding of bubbling phenomena, and help optimize bubbler configuration.

Plenum space temperature and estimation of Q_U

Commercial melters are typically heated by burning fuel above the melt [26, 27, 28]. According to Trier [26], the heat supplied to the batch in commercial melters operating in the 1400 to 1600°C temperature range is typically 45 to 80 kW·m^{-2}. In Joule-heated waste glass melters, the heat for melting is generated by electric power dissipation in molten glass. Plenum space temperature typically ranges from 400 to 600°C and the heat flux from plenum space can be estimated as Q_U = ~ 10 kW m^{-2}. As this low heat flux evaporates only a fraction of water charged with the feed, a substantial portion of the cold cap surface is covered by boiling slurry. In the waste glass melter equipped with plenum heaters, the plenum space temperature ranges from 700 to 900°C and Q_U = ~ 30 kW m^{-2} [29, 30]. Exposing the cold cap surface to such a high heat flux results in complete evaporation of slurry feed water in a small area under the feed nozzle, while most of the feed surface is dry and hot. According to Equation (1), the melting rate increases as Q_U increases (Figure 6). In waste glass melters that are not equipped with plenum heaters, heat radiates from molten glass to the plenum space and back to the cold cap. Bubblers increase Q_U by bringing hot melt to the surface and by creating and enlarging vent holes, thus increasing the surface temperature and the free surface area of the melt. Yet, as Matlack et al. [25] reported, the plenum temperature of a large-scale melter did not change considerably with changing bubbling rate, as it is dominated solely by the cold cap surface coverage and the molten glass temperature. The effect of bubbling on the Q_U is minor in comparison with the impact of plenum heaters.

It should be noted that, without the complete model of the waste glass melter, it is not possible to estimate Q_U. Thus, Q_U is currently a model parameter, which will be computed once the cold cap model is implemented in the full melter model.

Comparison of model results with experimental data

Experimental melter tests were performed at various scales and melter operating conditions with high-alumina feed of which A0 is a simplified version [31]. The reported steady-state average melting rates with strong bubbling were 700 kg·m^{-2} day^{-1} at T_M = 1150°C and 1200 kg·m^{-2} day^{-1} at T_M = 1200°C [31]. In both cases, the cold cap bottom temperature, T_B, was approximately 50°C lower than the T_M.

Figure 12 compares the simulation results with measured rates of melting plotted against $T_B \approx T_M - 50$°C [31]. Simulations were performed assuming no secondary foam (Φ = 1) and Q_U = 12 kW·m^{-2}, which is likely to exist when the plenum space temperature is ~450°C; this temperature was measured during melter tests and was independent of the T_M [31]. The melting rate was computed solely using feed properties and melter operating conditions without any fitting parameters. The nearly perfect agreement between measured and computed melting rates for T_M = 1150°C is rather fortuitous. The difference between the measured and computed values for T_M = 1200°C is noticeable, but its significance cannot be judged because of a lack of additional data. More importantly, the slope of the line in Figure 12, ~ 0.90 % per K, is in a good agreement with the observation [31] that, for most tests at constant bubbling, the melting rate increases approximately 1 % per K.

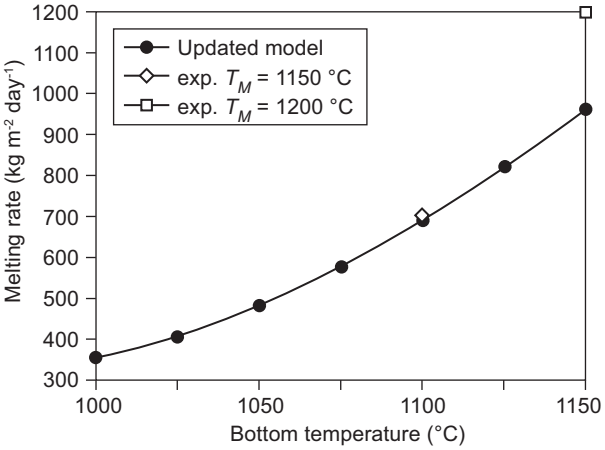

Figure 12. Comparison of melting rate measured experimentally [31] and predicted by the cold cap model (assuming Q_U = 12 kW m^{-2} and no secondary foam).

CONCLUSIONS

The updated cold cap model, which estimates melting rate solely as a function of feed properties and melter operating conditions (no fitting parameters are used), can be considered a good tool for the understanding of the effect of bubbling on the melting rate. We separately examined the different bubbling effects, and suggest that the melting rate in a Joule-heated waste glass melter is mainly enhanced via forced convection introduced by bubblers. The forced convection brings hot molten glass to the cold cap bottom, thus increasing the heat flux needed for the feed-to-glass conversion. Other effects, such as stirring of the feed from the cold cap into the molten glass or displacing secondary foam, also play a role.

The results obtained using the current cold cap model are in reasonable agreement with data from experimental melter studies, especially for lower bubbling rates. However, both secondary foam and cavity layer can be displaced when intense bubbling is applied. In such case, the hot molten glass comes in a direct contact with the primary foam of the reacting feed, significantly increasing the heat transfer to the cold cap. To account for this phenomenon, additional mathematical formulation is needed for the kinetics of primary foam expansion and collapse.

Finally, the cold cap bottom temperature and the heat flux from above, which are treated as boundary conditions, will become computed outputs after the cold cap model is implemented into the model of the whole glass melter.

Acknowledgements

This work was supported by the U.S. Department of Energy's Waste Treatment and Immobilization Plant Federal Project Office under the direction of Dr. Albert A. Kruger. Richard Pokorny acknowledges financial support from the specific university research (MSMT No 20/2014). The authors are grateful to Jaehun Chun for insightful discussions and Dong-Sang Kim for kindly providing the diagram shown in Figure 3. Pacific Northwest National Laboratory is operated for the U.S. Department of Energy by Battelle.

REFERENCES

1. Kirkbride R.A., Allen G.K., Orme R.M., Wittman R.S., Baldwin J.H., Crawford T.W., Jo J., Fergestrom L.J., Hohl T.M., Penwell D.L.: *Tank waste remediation system operation and utilization plan*, Vol. I, HNF-SD-WM-SP-012, Numatec Hanford Corporation, Richland, Washington 1999.
2. Pokorny R., Hrma P.: J. Nucl. Mater. *445*, 190 (2014).
3. Choudhary M.K., Venuturumilli R., Hyre M.R.: Int. J. Appl. Glass Sci. *1,* 88 (2010).
4. Perez J.M., Chapman C.C., Mohr R.K., Matlack K.S., Pegg I.L. In: Proceedings for ICEM'05: The 10th International Conference on Environmental Remediation and Radioactive Waste Management, September 4–8, 2005, Glasgow, Scotland.
5. Matlack K.S., Gong W., Bardakci T., D'Angelo N., Lutze W., Callow R.A., Brandys M., Kot W.K., Pegg I.L.: *Integrated DM1200 Melter Testing of Bubbler Configurations Using HLW AZ-101 Simulants*, VSL-04R4800-4, Vitreous State Laboratory, The Catholic University of America, Washington, DC, 2004.
6. Matlack K.S., Gan H., Chaudhuri M., Kot W., Gong W., Bardakci T., Pegg I.L., Innocent J.: *DM100 and DM1200 melter testing with high waste loading glass formulations for Hanford high-aluminum HLW streams*, VSL-10R1690-1, Vitreous State Laboratory, The Catholic University of America, Washington, DC 2010.
7. Pokorny R., Hrma P.: J. Nucl. Mater., *429*, 245 (2012).
8. Chapman C.: *Investigation of Glass Bubbling and Increased Production Rate*. REP-RPP-069, Duratek, Richland, Washington 2004.
9. Agarwal V., Guillen D. P.: *Incorporating Cold Cap Behavior in a Joule-Heated Waste Glass Melter Model*, INL-13-29794, Idaho Falls, ID 2013.
10. Schweiger M.J., Hrma P., Humrickhouse C.J., Marcial J., Riley B.J., TeGrotenhuis N.E.: J. Non-Cryst. Solids *356*, 1359 (2010).
11. Pokorny R., Rice J.A., Schweiger M.J., Hrma P.: J. Am. Ceram. Soc. *96*, 1891 (2013).
12. Rice J.A., Pokorny R., Schweiger M.J., Hrma P.: J. Am. Ceram. Soc. *97*, 1952 (2014).
13. Hrma P., Schweiger M.J., Humrickhouse C.J., Moody J.A., Tate R.M., Rainsdon T.T., TeGrotenhuis N.E., Arrigoni B.M., Marcial J., Rodriguez C.P., Tincher B.H.: Ceram.-Silik. *54*, 193 (2010).
14. Pokorny R., Rice J.A., Crum J.V., Schweiger M.J., Hrma P.: J. Nucl. Mater. *443*, 230 (2013).
15. Pokorny R., Pierce D.A, Hrma P.: Thermochim. Acta *541*, 8 (2012).
16. Chun J., Pierce D.A., Pokorny R., Hrma P.:Thermochim. Acta *559*, 32 (2013).
17. Matlack K.S., Kot W.K., Brandys M., Nelson C., Schatz T.R., Gong W., Pegg I.L.: *Start-Up and Commisioning Tests on the DuraMelter 1200 HLW pilot Melter System Using AZ-101 HLW Simulants*, VSL-01R0100-2, Vitreous State Laboratory, The Catholic University of America, Washington, DC 2001.
18. Hrma P.: J. Colloid Interf. Sci. *134*, 161 (1990).
19. Bikerman J.J.: Trans. Faraday Soc. *34*, 634 (1948).
20. Hrma P.: Glastech. Ber. *63*, 360 (1990).
21. Henager S.H., Hrma P., Swearingen K.J., Schweiger M.J., Marcial J., TeGrotenhuis N. E.: J. Non-Cryst. Solids *357*, 829 (2011).
22. Kim D-S., Hrma P.: Ceram. Bull. *69*, 1039 (1990).
23. Kim D-S., Hrma P.: J. Am. Ceram. Soc. *74*, 551 (1991).
24. Hrma P., Kim D-S.: Glass Technol. *35*, 128 (1994).
25. Matlack K.S., Kot W.K., Callow R.A., Joseph I., Pegg I.L.: *Testing of optimized bubbler configuration for HLW Melter*, VSL-13R2950-1, Vitreous State Laboratory, The Catholic University of America, Washington, DC 2013.
26. Trier W.: *Glass Furnaces: Design, Construction and Operation*, p. 134-138, Society of Glass Technology, Sheffield, 1987. ISBN: 0900682205.
27. Fan T.-H., Fedorov A. G.: J. Quant. Spectrosc. Radiat. Transfer *73*, 285 (2002).
28. Wang J., Brewster B.S., Webb B.W., McQuay M.Q.: J. Energy Inst. *78*, 117 (2005).
29. Guerrero H.N., Bickford D.F.: *Numerical Models of Waste Glass Melters Part I – Lumped Parameter Analyses of DWPF*, WSRC-MS-2003-00272 Part I, Westinghouse Savannah River Co., Aiken 2003.
30. Guerrero H.N., Bickford D.F., Naseri-Neshat H.: *Numerical Models of Waste Glass Melters Part II - Computational Modeling of DWPF*, WSRC-MS-2003-00272 Part II, Westinghouse Savannah River Co., Aiken, 2003.
31. Matlack K.S., Gan H., Chaudhuri M., Kot W.K., Gong W., Bardakci T., Pegg I.L., Joseph I.: *Melt Rate Enhancement for High Aluminum HLW Glass Formulations*, VSL-08R1360-1, Vitreous State Laboratory, The Catholic University of America, Washington, DC 2008.